39th IAHR WORLD CONGRESS GRANADA, SPAIN 2022 From Snow to Sea 19-24 June 2022

Proceedings of the 39th IAHR World Congress
19–24 June 2022, Granada, Spain
doi://10.3850/IAHR-39WC2521716X20221011

Depth-resolved Modelling of Suspended Sediment in the Surf and Swash Zones

Joost W.M. Kranenborg[(1)], Geert H.P. Campmans[(1)], Jebbe J. van der Werf[(1,2)], Robert T. McCall[(2)], Niels Gjøl Jacobsen[(3)], Ad J.H.M. Reniers[(4)], Suzanne J.M.H. Hulscher[(1)]

[(1)] University of Twente, Enschede, The Netherlands
j.w.m.kranenborg@utwente.nl
[(2)] Deltares, Delft, The Netherlands
[(3)] Vattenfall Vindkraft, Denmark
[(4)] Delft University of Technology, Delft, The Netherlands

Abstract

We present a depth-resolving model that is capable of resolving the vertical flow and suspended sediment structures in the surf and in the swash zones. The model uses the RANS equations to simulate hydrodynamics, and includes sediment transport using an advection diffusion approach. The model is first validated hydrodynamically using measured surface elevations. The results from the model show a strong vertical dependence in the suspended sediment flux, and that at certain cross-shore locations the wave-averaged sediment transport moves onshore where the average flow velocity is offshore-directed. These physical processes are important to consider when designing more practical, long-term depth-averaged models for simulating coastal morphodynamics.

Keywords: Swash-zone; Numerical model; Sediment transport; Morphodynamics; Waves

1. INTRODUCTION

The swash zone defines the cross-shore region where waves run up and down the beach. This region is characterized by strong flows, high amounts of turbulence, large sediment fluxes and rapid morphological changes. These characteristics make it an important region for understanding the development of the beach in general. Even though it is easily accessible, the dynamic nature makes it difficult to study experimentally. For this reason, numerical models are developed to increase our understanding of the relevant processes, and ultimately better predict the shoreline evolution.

At present, most numerical models capable of modelling morphodynamics in the swash zone are based on a depth-averaged approach. These models can reproduce the depth-averaged hydrodynamics but have difficulty modelling sediment transport and morphodynamics. This has been attributed to different modelling aspects, from the use of wave-averaged transport formulations to missing processes such as turbulence and vertical structures in the suspended sediment concentration (Mancini et al., 2021; Ruffini et al., 2020). Depth-resolving models are not hampered by these assumptions, and allow inclusion of detailed formulations for turbulence. Therefore, these models are potentially a great tool to investigate the importance of these vertical processes.

In this paper we give a brief presentation of how depth-resolving models give insights into how suspended sediment is transported in the water column. Specifically, we will look at wave-averaged velocities and sediment fluxes over multiple modelled wave groups. First, we briefly introduce the model background and setup, and describe the experimental case we compare with. Then we validate the model using measured and modelled surface elevations, after which we show the modelled wave-averaged flow velocities and sediment fluxes. Finally, we briefly discuss and summarize the results and present an outlook for future research.

2. METHODOLOGY

In this study we will use a model developed in the OpenFOAM® environment, based on the model by Jacobsen et al., (2014). To validate the model, we will compare modelled output with the experiments by van der Zanden et al., (2019). In this section, both the model setup and the dataset used are described.

2.1 Model Description

For simulating hydrodynamics, the model uses the 2DV Reynolds Averaged Navier-Stokes (RANS) equations, coupled with a Volume of Fluid (VoF) approach to account for air and water in the model domain. Specifically, we use the isoAdvector approach (Roenby et al., 2016). Furthermore, a $k-\omega$ equation as proposed by Wilcox (2008) is used, including the limiter suggested by Larsen & Fuhrman (2018). For wave-generation, the waves2Foam package (Jacobsen et al., 2012) is used together with the OceanWaves3D package (Engsig-Karup et al., 2009; Paulsen et al., 2014) to generate the waves. The boundary conditions at the bed are set to model a rough boundary with a roughness height $K_n = 2.5D_{50}$. For velocity we set a no-slip condition at the bed boundary and for k and ω the boundary conditions we use the approach by Fuhrman et al. (2010). The boundary layer in the bottom cell is accounted for using the generalized wall-function approach as described by Larsen et al. (2017).

Sediment transport is modelled using separate transport formulations for bedload and suspended load. In short, the bedload transport is calculated at the bed interface using the bed-shear stress and local bed slope (Engelund et al., 1976; Roulund et al., 2005). Suspended load is calculated using an advection-diffusion approach, with a reference concentration set at $2.5D_{50}$ above the bed, according to the formula by Engelund and Fredsøe (1976). In the present study, the bed is kept static. More details on the implementation can be found in the original model paper (Jacobsen et al., 2014).

The model consists of just over 1 million cells, which mostly are 2x2 cm^2 in size. Close to the bed the cells are smaller, decreasing to a thickness of 0.5 mm in the vertical direction. The solver was run in parallel on 24 processors.

2.2 Data Description

The data used in this study was gathered in the CIEM facility in Barcelona (van der Zanden et al., 2019). The flume is 100 m long, 4.5 m deep and 3 m wide. The flume was filled until it was 2.5 m deep at the paddle location. At the other side of the flume, a beach with an initial slope of 1:15 was built using medium sand ($D_{50} = 0.25\ mm$). Because the experiment consisted of many subsequent wave runs, the initial bed used in this study had already deformed from its initial 1:15 profile, on which breaker bars and a concave swash profile had formed. More information about the profile evolution can be found in Eichentopf et al., (2019). We use the measurements of bichromatic waves with the group frequency $T_{gr} = 14.8\ s$, and wave components $f_1 = 2T_{gr}/7$ and $f_2 == 2T_{gr}/9$, which both had wave amplitudes of $H_1 = H_2 = 0.32$ m. This leads to a total wave signal that forms two alternating wave groups which repeat every $2T_{gr}$ seconds.

The experiments featured various measuring equipment. In this study we use some of the wave gauges to compare measurements of the surface elevation with the model. For this comparison, we use the Root Mean Square Error (RMSE) to quantify the difference, both in a non-normalized sense and normalized by the range (i.e. the maximum minus the minimum) of the signal. Furthermore, we define the cross-shore coordinate x, defined as the distance shoreward of the wave paddle, and the y coordinate as the vertical distance above the initial still water line, or the bed where the initial bed would be exposed.

3. RESULTS

3.1 Validation

The model is first validated for hydrodynamics. This is done by comparing measurements of the surface elevation of the flume measurements and the model. We used two locations; one in the surf-zone before the wave breaks ($x = 57.82$ m) and one in the swash-zone ($x = 77.55$ m). The comparison can be seen in Figure 1. The RMSE for the surface elevations are 0.06 m, 0.02 m for the surf and swash location, respectively. This amounts to roughly 8% and 11% of the range of the measured surface elevations. One source of this deviation is that the model actively absorbs reflected waves, whereas no wave absorption was present at the experimental campaign. Furthermore, the transformation of the paddle signal to a velocity signal used in OcenWaves3D also introduces errors. We consider the surface elevations to be modelled with reasonable accuracy. For instance, the two alternating wave-groups are clearly visible both in the experimental and modelled results.

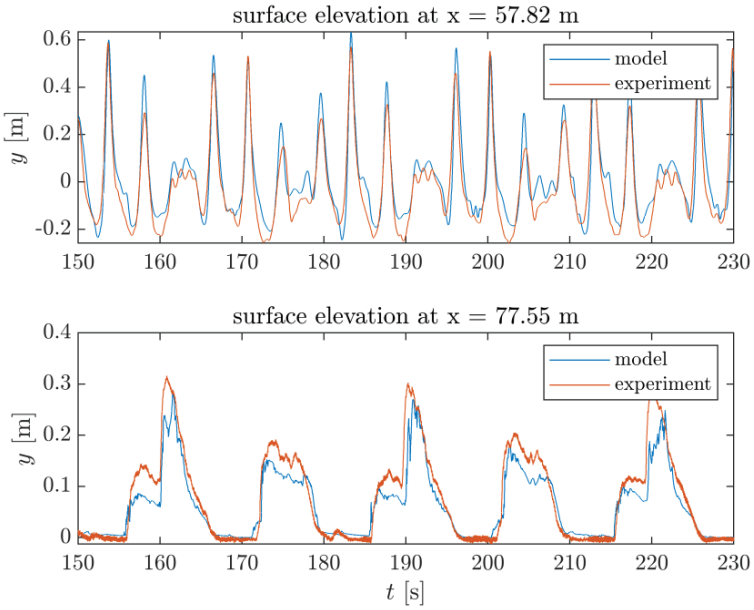

Figure 1. Comparison of measured and modelled surface elevations at two different locations in the flume.

3.2 Wave-averaged Sediment Flux

Figure 2 shows the time-averaged cross-shore velocity and the time-averaged cross-shore sediment advection over six wave-group periods (from t = 135 s to t = 223.8 s). The averaged velocities show a clear undertow pattern, where the average velocity is onshore-directed at higher elevations, and offshore-directed at lower elevations. The strongest average velocities occur just landward wave-breaking, around x = 66 m to x = 73 m.

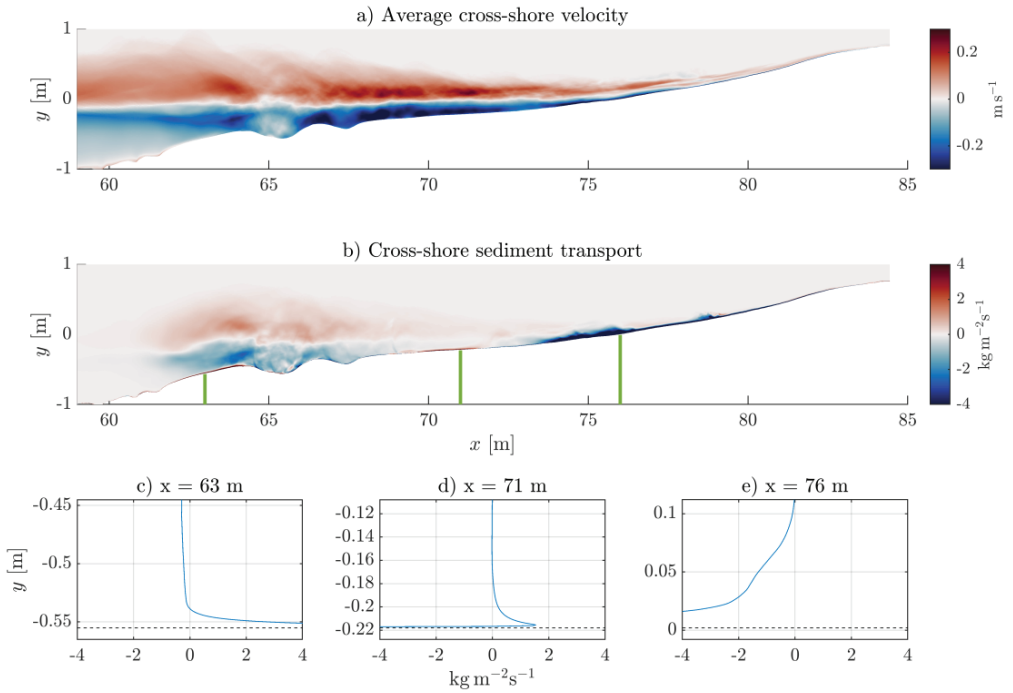

Figure 2. a) Time-averaged velocities and b) sediment fluxes in the cross-shore direction. The green lines show the cross-shore locations of the subsequent panels c-e. These panels show vertical profiles of the cross-shore sediment transport at three different locations. The dashed lines in panels (c)-(e) indicate the bed levels.

Looking at cross-shore sediment transport, we see some different phenomena. Firstly, from around x = 62 m to x = 73 m, we see a similar pattern as with the averaged velocities. Here at higher elevations suspended sediment is transported onshore and at lower elevations it is transported offshore. The onshore sediment transport happens due to waves picking up sediment higher up in the water column, and transporting this onshore as the wave breaks. Further onshore in the swash zone, from around x = 70 m, an additional onshore transport of sediment close to the bed can be observed (see panel (d)). This happens as the flow and turbulence associated with a collapsed wave interacts with the bed, resulting in large sediment pickup and advection at this location. Even further onshore, at around x = 75 m, strong offshore sediment fluxes are observed (see panel (e)). This transport happens during the backwash, and happens in the region where strong sheet flow was observed (van der Zanden et al., 2019).

At around *x* = 75 m, we see the importance of wave-swash interactions, where in this case sediment is briefly picked up by the collision of an incoming wave and the backwash. Figure 3 shows in more detail what happens during such a collision. Here, large offshore transport in this region is associated with high levels of turbulence. The net effect of these collisions in the simulations leads to offshore-directed sediment transport.

Lastly, just above the breaker bar between x = 61 m and x = 64 m, a region of strong onshore directed sediment transport is observed (see panel (c)). This onshore transport happens as a shoaling wave travelling over the bar quickly accelerates the flow shoreward, transporting sediment shoreward. During the backwash, the stronger returning currents appear higher in the water column and therefore do not transport much sediment offshore.

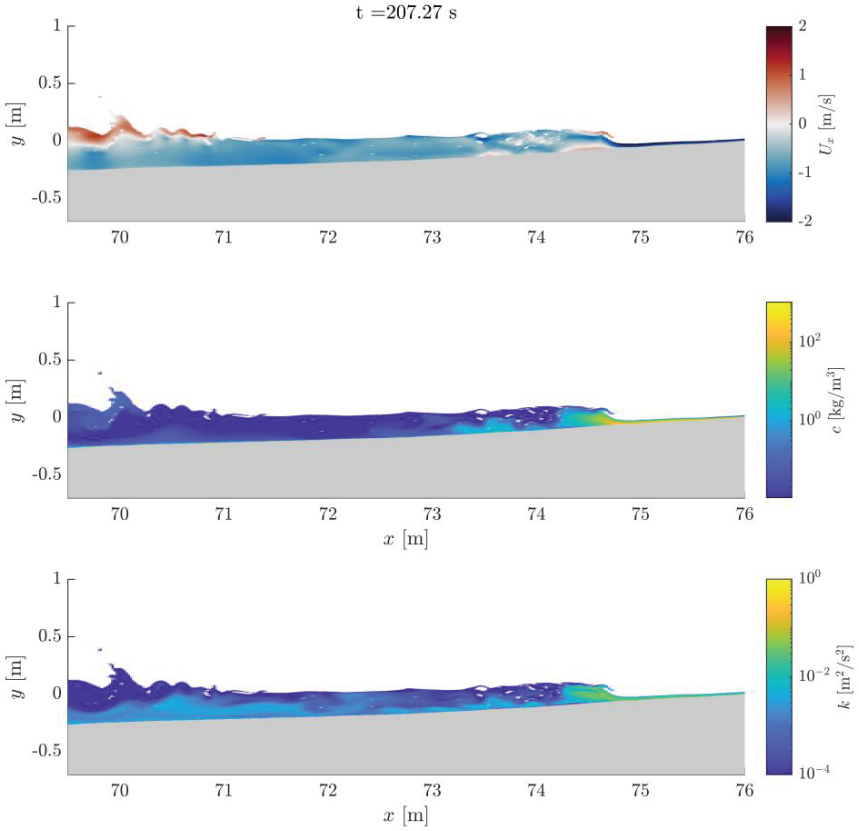

Figure 3. Snapshot of cross-shore velocity, instantaneous suspended sediment concentration and instantaneous turbulent kinetic energy.

4. DISCUSSION AND CONCLUSION

There are some important differences between the model and the measurements that can influence the results. For instance, the present study has only been conducted using a model that does not dynamically move the bed. This is an important process, as measurements have shown that the bed can move several

centimeters within seconds in strong swash currents (van der Zanden et al., 2015). Even though this particular case was chosen for its relatively small morphodynamic change over the full measurement duration, the impact of intraswash morphodynamics on the modelled sediment fluxes should still be investigated.

Furthermore, the model actively damps the reflected waves, whereas no active wave absorption was applied during the experiments. These two effects mean that slight differences in hydrodynamical forcing on the beach are expected. However, the validation shows that these effects are relatively unimportant and that the general motion of the swash is accounted for.

The results presented here show a glimpse of what depth-resolving models can offer as a tool for detailed investigation into sediment fluxes in the surf and swash zones. The presented model shows some interesting phenomena that are important for the total flux of sediment transport, but that are not easily captured by depth-averaged models. In the future, we aim to investigate the importance of these processes for net sediment transport and suggest how such processes can be accounted for in depth-averaged models.

5. ACKNOWLEDGEMENTS

This work is part of the research program Shaping The Beach with project number 16130, which is financed by the Netherlands Organisation for Scientific Research (NWO), with in-kind support by Deltares. This work was carried out on the Dutch national e-infrastructure with the support of SURF Cooperative.

6. REFERENCES

Eichentopf, S., van der Zanden, J., Cáceres, I., & Alsina, J. M. (2019). Beach Profile Evolution towards Equilibrium from Varying Initial Morphologies. *Journal of Marine Science and Engineering*, *7*(11), 406. https://doi.org/10.3390/jmse7110406

Engelund, F., Fredsøe, J., Fredsoe, J., & Fredsøe, J. (1976). A Sediment Transport Model for Straight Alluvial Channels. *Hydrology Research*, *7*(5), 293–306. https://doi.org/10.2166/nh.1976.0019

Engsig-Karup, A. P., Bingham, H. B., & Lindberg, O. (2009). An efficient flexible-order model for 3D nonlinear water waves. *Journal of Computational Physics*, *228*(6), 2100–2118. https://doi.org/10.1016/j.jcp.2008.11.028

Fuhrman, D. R., Dixen, M., & Jacobsen, N. G. (2010). Physically-consistent wall boundary conditions for the k-turbulence model. *Journal of Hydraulic Research*, *48*(6), 793–800. https://doi.org/10.1080/00221686.2010.531100

Jacobsen, N. G., Fredsoe, J., & Jensen, J. H. (2014). Formation and development of a breaker bar under regular waves. Part 1: Model description and hydrodynamics. *Coastal Engineering*, *88*, 182–193. https://doi.org/10.1016/j.coastaleng.2013.12.008

Jacobsen, N. G., Fuhrman, D. R., & Fredsøe, J. (2012). A wave generation toolbox for the open-source CFD library: OpenFoam®. *International Journal for Numerical Methods in Fluids*, *70*(9), 1073–1088. https://doi.org/10.1002/fld.2726

Larsen, B. E., & Fuhrman, D. R. (2018). On the over-production of turbulence beneath surface waves in Reynolds-averaged Navier-Stokes models. *Journal of Fluid Mechanics*, *853*, 419–460. https://doi.org/10.1017/jfm.2018.577

Larsen, B. E., Fuhrman, D. R., Baykal, C., & Sumer, B. M. (2017). Tsunami-induced scour around monopile foundations. *Coastal Engineering*, *129*(August), 36–49. https://doi.org/10.1016/j.coastaleng.2017.08.002

Mancini, G., Briganti, R., McCall, R., Dodd, N., & Zhu, F. (2021). Numerical modelling of intra-wave sediment transport on sandy beaches using a non-hydrostatic, wave-resolving model. *Ocean Dynamics*, *71*(1), 1–20. https://doi.org/10.1007/s10236-020-01416-x

Paulsen, B. T., Bredmose, H., & Bingham, H. B. (2014). An efficient domain decomposition strategy for wave loads on surface piercing circular cylinders. *Coastal Engineering*, *86*, 57–76. https://doi.org/10.1016/J.COASTALENG.2014.01.006

Roenby, J., Bredmose, H., & Jasak, H. (2016). A computational method for sharp interface advection. *Royal Society Open Science*, *3*(11), 160405. https://doi.org/10.1098/rsos.160405

Roulund, A., Sumer, B. M., Fredsøe, J., & Michelsen, J. (2005). Numerical and experimental investigation of flow and scour around a circular pile. *Journal of Fluid Mechanics*, *534*, 351–401. https://doi.org/10.1017/S0022112005004507

Ruffini, G., Briganti, R., Alsina, J. M., Brocchini, M., Dodd, N., & McCall, R. (2020). Numerical Modeling of Flow and Bed Evolution of Bichromatic Wave Groups on an Intermediate Beach Using Nonhydrostatic XBeach. *Journal of Waterway, Port, Coastal, and Ocean Engineering*, *146*(1), 04019034. https://doi.org/10.1061/(ASCE)WW.1943-5460.0000530

van der Zanden, J., Alsina, J. M., Cáceres, I., Buijsrogge, R. H., & Ribberink, J. S. (2015). Bed level motions and sheet flow processes in the swash zone: Observations with a new conductivity-based concentration measuring technique (CCM +). *Coastal Engineering*, *105*, 47–65.

https://doi.org/10.1016/j.coastaleng.2015.08.009
van der Zanden, J., Cáceres, I., Eichentopf, S., Ribberink, J. S., van der Werf, J. J., & Alsina, J. M. (2019). Sand transport processes and bed level changes induced by two alternating laboratory swash events. *Coastal Engineering*, *152*, 103519. https://doi.org/10.1016/j.coastaleng.2019.103519
Wilcox, D. C. (2008). Formulation of the k-ω turbulence model revisited. *AIAA Journal*, *46*(11), 2823–2838. https://doi.org/10.2514/1.36541

